Cell Stem Cell, Volume *25*

Supplemental Information

Oligodendrocyte Death in Pelizaeus-Merzbacher Disease Is Rescued by Iron Chelation

Hiroko Nobuta, Nan Yang, Yi Han Ng, Samuele G. Marro, Khalida Sabeur, Manideep Chavali, John H. Stockley, David W. Killilea, Patrick B. Walter, Chao Zhao, Philip Huie Jr., Steven A. Goldman, Arnold R. Kriegstein, Robin J.M. Franklin, David H. Rowitch, and Marius Wernig

Supplemental Figure 1, Related to Figure 1

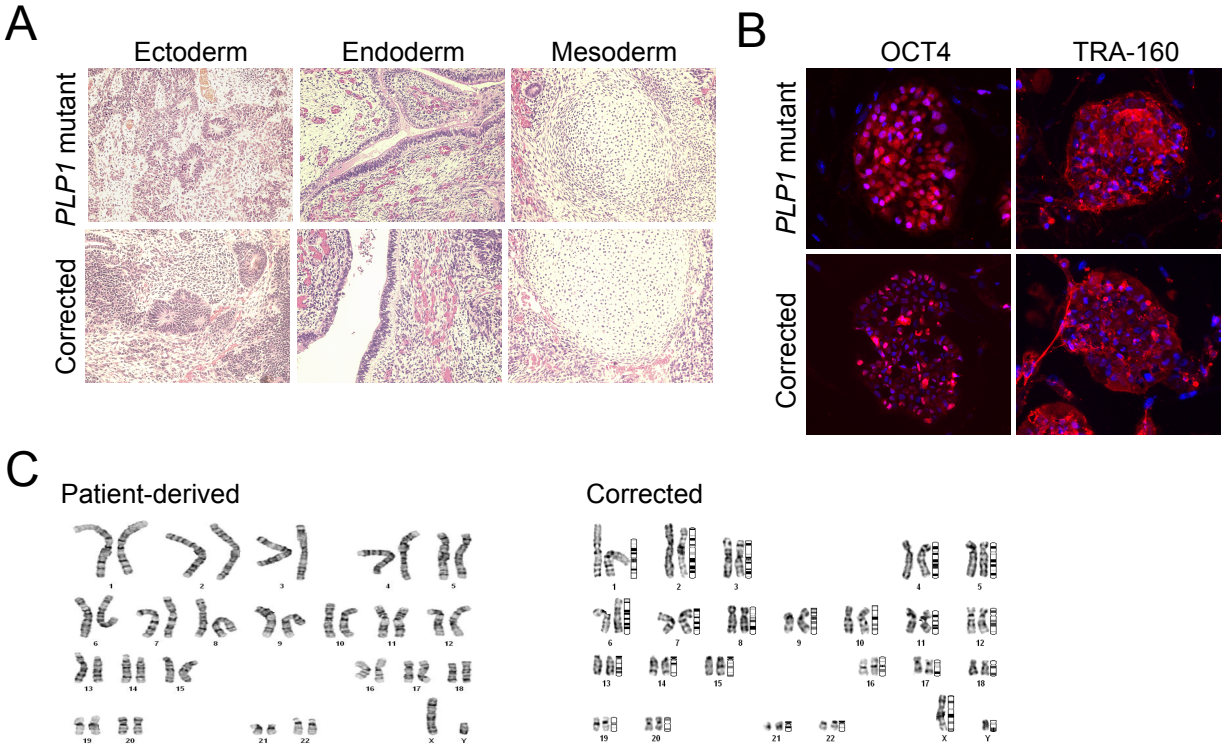

Supplemental Figure 2, Related to Figure 1

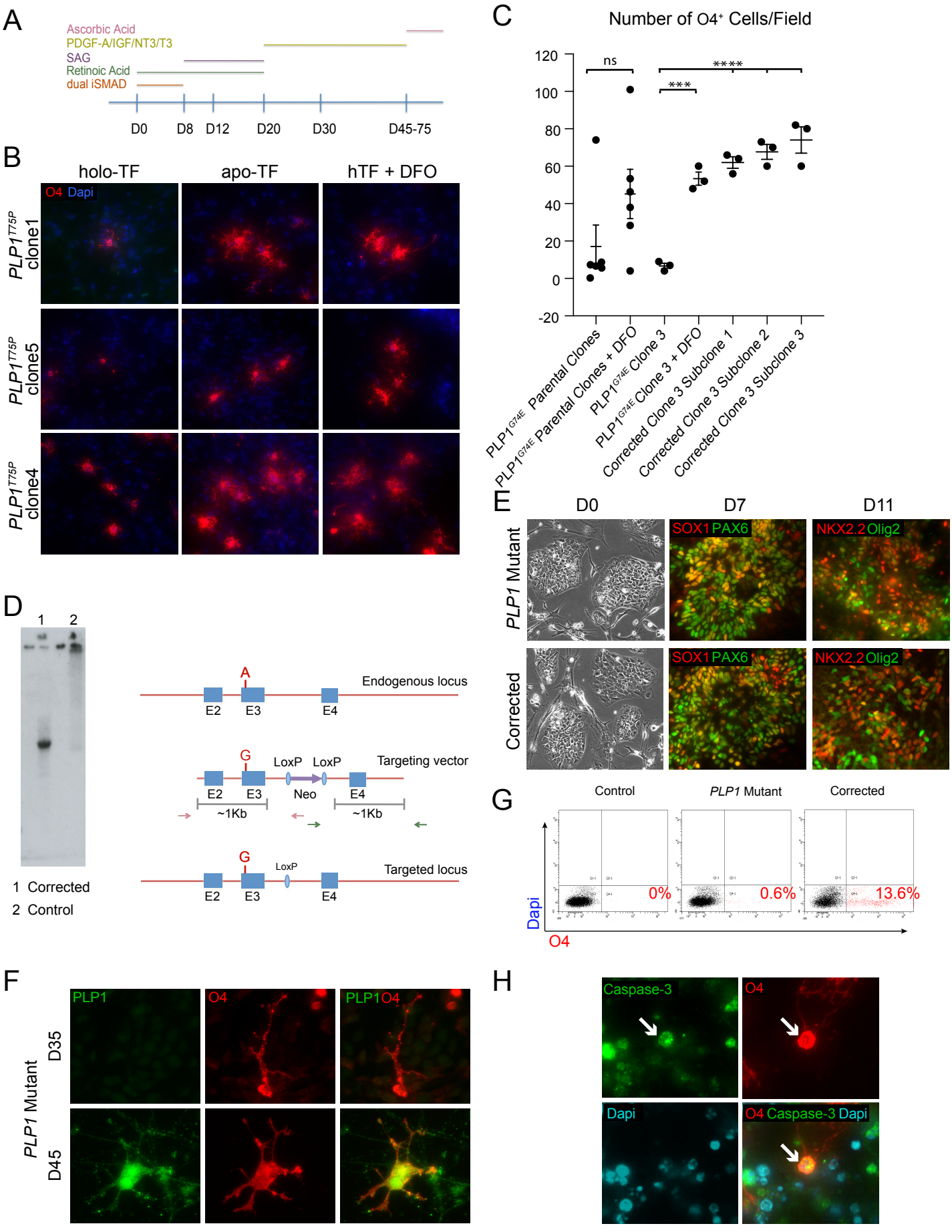

Supplementary Figure 3, Related to Figure 3

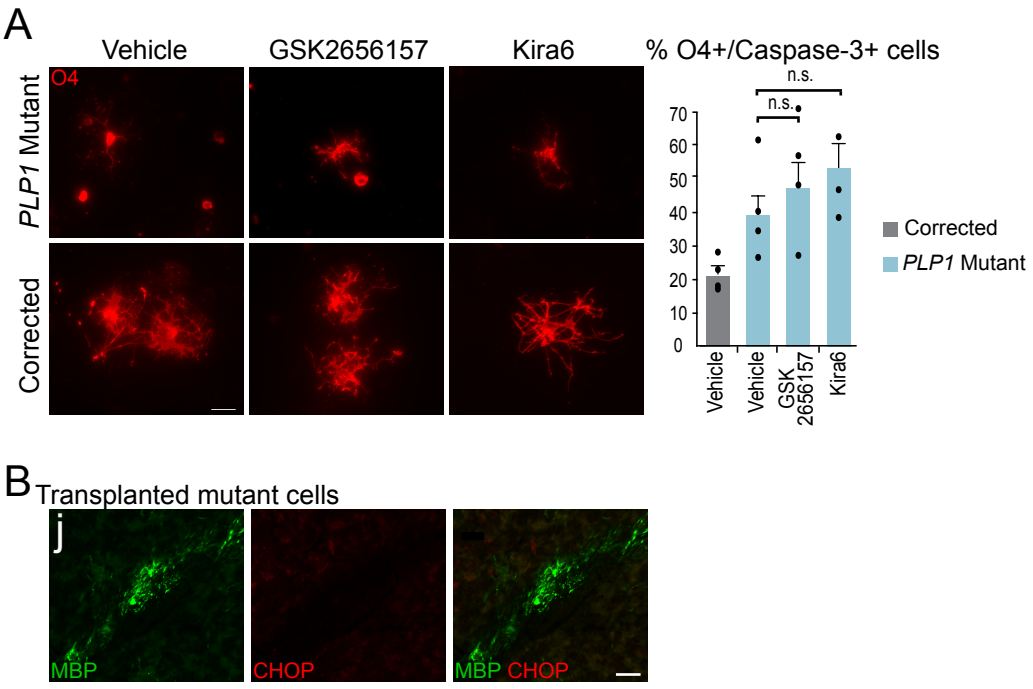

Supplementary Figure 4, Related to Figure 5

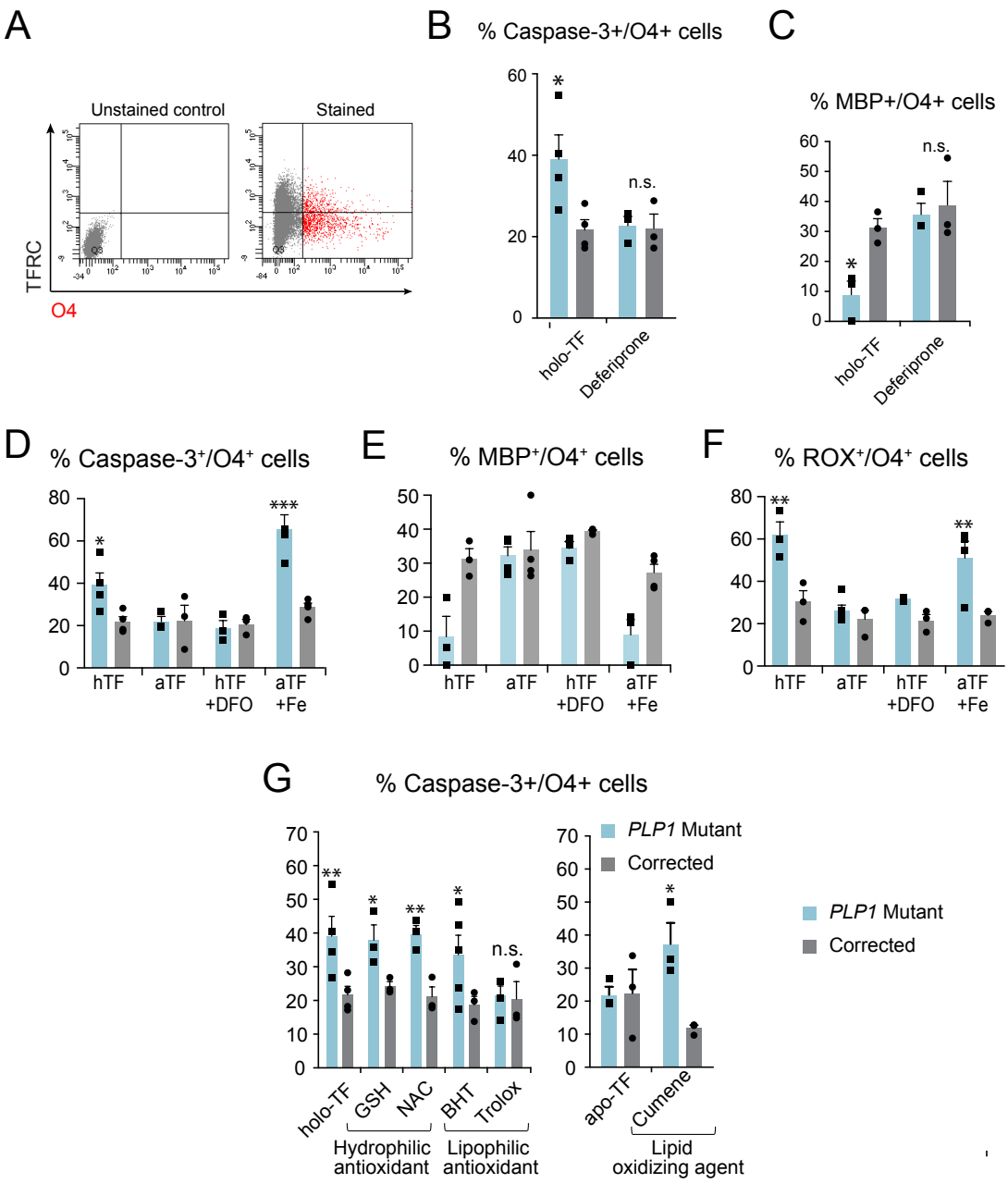

Supplemental Figure 5, Related to Figure 7

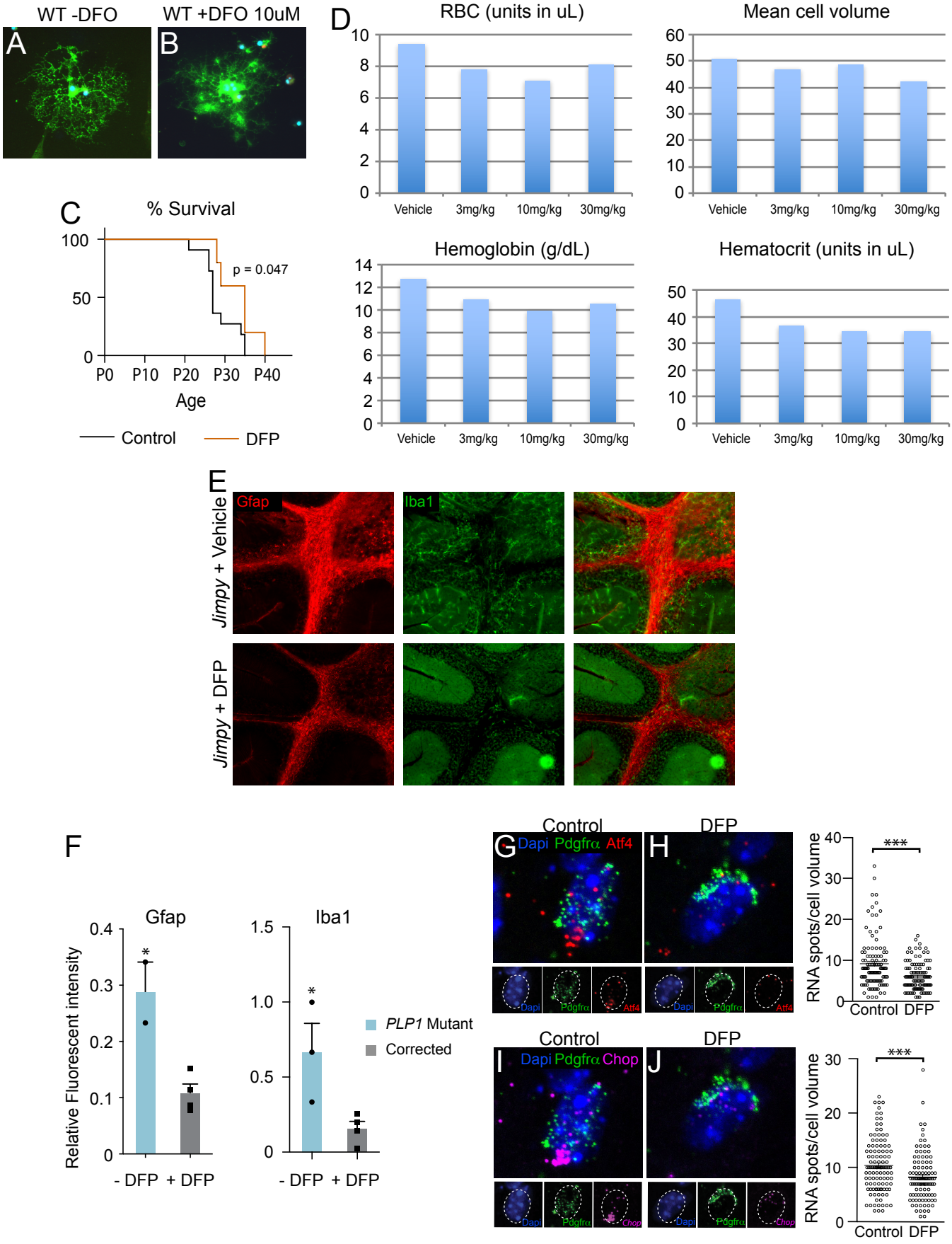

Supplemetary Table 1, Related to STAR Methods

Primer sequences for quantitative PCR.

PAX6 FW: TTTGCCCGAGAAAGACTAGC RV: CATTTGGCCCTTCGATTAGA
OLIG2 FW: TGCGCAAGCTTTCCAAGAT RV: CAGCGAGTTGGTGAGCATGA
SOX1 FW: GGAATGGGAGGACAGGATTT RV: AACAGCCGGAG CAGAAGATA
NKX2.2 FW: GACAACTGGTGGCAGATTTCGCTT RV: AGCCACAAAGAAAGGAGTTGGACC
Spliced XBP1 FW: CTGAGTCCGCAGCAGGTGCAG RV: GGTCCAAGTTGTCCAGAATGCCC
BIP FW: CCGCTGAGGCTTATTTGGGA RV: TCTTTGGTTGCTTGGCGTTG
ATF3 FW: CTCGGGGTGTCCATCACAAA RV: TTGTTTCGGCACTTTGCAGC
HMOX1 FW: GAGGAACTTTCAGAAGGGCCA RV: CCTTGTTGCGCTCAATCTCC
SOD3 RW: GTGCAGCTCTCTTTTCAGGAG RV: GAGCAGGCAGGAACACAGTAG
ATOX1 FW: CGGGTCCTCAATAAGCTTGGA RV: AGGGTTGCAAGCAGAGTGTC
SCARA3 FW: CCGAAGACATCTCCTTGACCC RV: GCAGTTGTTCAGGGCTTTCG
TXNIP RW: ACCTGCGCTATGAAGACACG RV: AAGCTCAAAGCCGAACTTGT
SOD2 FW: GTTGGGGTTGGCTTGGTTTC RV: CCCCAGCAGTGGAATAAGGC
TXN FW: GGACGCTGCAGGTGATAAAC RV: CGTTGGAATACTTTTCAGAGAGGG
TXNRD2 FW: ATGATCTCCTGGTGGTCGGC RV: TGGGGAGAAGGTTCCACGTA
TF FW: GATGCTTACCTGGCTCCCAATAAC RV: CTTCTTCACCACAGCAACAGCAT
IRP1 FW: CTTGGGTCAGGTTCGCCG RV: TCCAGGATGGTGGAAACTGC
IRP2 FW: GGCAGAAATCGAGAGAGGCT RV: TGAGCCATTCCAGTTCCAGG
TFRC FW: TTGGACATGCTCATCTGGGG RV: CCTGATGACCGAGATGGTGG
APP FW: GATCCCAAGAAAGCCGCTCA RV: CACTGCAGGCACGTTGTAGA
CP FW: AGCTGGAACAGAGGATTCTGC RV: GACAAACAATCAGGGGGCCA
P53 FW: ACCTATGGAAACTACTTCCTGAAAA RV: CAATATCGTCCGGGGACAGC
SAT1 FW: CAGTGACATACTGCGGCTGAT RV: AGGGGTGCTCTCCAAAACC
PLP1 FW: TATCTCATCAATGTGATCCATGCCT RV: TCCTAGCCATTTTCCCAAACAAT
DM20 FW: TATCTCATCAATGTGATCCATGCCT RV: CCACAAACGTTGCGCTCA

Supplementary Figure 1. Related to Figure 1. Validation of pluripotency and normal karyotype in *PLP1*^{G74E} patient and corrected iPSCs. A, Subcutaneous injection of iPSCs in immunodeficient mice resulted in teratoma with three germ layers: ectoderm, endoderm, mesoderm. **B**, iPSCs express pluripotency markers OCT4 and TRA1-160 at the protein level. **C,** Both patient and corrected iPSCs show normal karyotype.

Supplementary Figure 2. Related to Figure 1. Oligodendrocyte differentiation kinetics of *PLP1* mutants and corrected iPSCs. A, Schematic of oligodendrocyte differentiation protocol. **B**, An example of large variability among three original iPSC lines generated simultaneously from a patient with *PLP1*^{T75P} mutation, and their response to apo-TF and DFO. Clone 4 naturally made oligodendrocytes in response to standardized protocol, but clone 1 and 5 generated minimal number of oligodendrocytes. **C,** Two left data sets show six original iPSC clonal lines generated from a patient with *PLP1*^{G74E} mutation and their response to DFO treatment showing large variability, resulting in non-significant difference. Five datasets to the right show the phenotypic results of the clone 3 used in the gene correction to WT *PLP1* sequence that generated multiple subclones (3 shown here) that share the same culture history, which resulted in a much smaller variability. **D**, (Left) Validation of a single genomic integration of the targeting construct by Southern blot. Lane 1 shows a single band of an appropriate size. (Right) Detailed targeting construct design for *PLP1*^{G74E} mutation. The mutant endogenous sequence contained a single base pair mutation in exon3. The targeting construct with homologous arms shown in gray contained wildtype sequence for correction purpose. It also contained neomycin resistant gene flanked by loxP sites for drug screening purpose. The targeting construct was cloned into AAV vector. After drug selection, targeted locus was sequenced using PCR product, which was amplified with primer pairs shown in pink and green. These primer pairs distinguish endogenous vs targeted sequence by amplifying a fragment containing human genomic DNA and newly introduced neomycin resistant gene. Homologously targeted clones were then transiently transfected with Cre recombinase to remove neomycin cassette. **E,** Initial phase of oligodendrocyte differentiation in both *PLP1*^{G74E} mutant and corrected cells are similar, assessed by iPSC morphology (D0), SOX1^{+}/PAX6^{+} neural rosette formation (D7), and NKX2.2^{+}/OLIG2^{+} oligodendrocyte precursors (D11). **F**, Onset of PLP1 protein expression in O4+ cells occurs between day 35 and 45. **G,** Representative FACS plots for quantification of O4+ cells. **H,** Representative images of Caspase-3, colocalizing with O4^{+} OPCs in *PLP1*^{G74E}.

Supplementary Figure 3. Related to Figure 3. Lack of rescue in *PLP1*^{G74E} OPCs by UPR/ER stress inhibitors. A, ER stress inhibitors GSK2656157 or Kira6 was added to the culture and surviving O4^{+} cells were quantified. The treatment did not rescue the mutant phenotype (N=3). **B**, Staining for ER stress marker CHOP in *Shiverer* mouse 12 weeks after transplantation of mutant cells shows no colocalization with transplanted oligodendrocytes (MBP^{+}).

Supplementary Figure 4. Related to Figure 5. Iron chelation treatment rescues defective mutant OPC differentiation. A, Representative FACS plot for transferrin receptor in O4+ oligodendrocytes. **B-C**, In addition to DFO treatment shown in Fig. 5 G-H, an additional iron chelator deferiprone showed beneficial effects in the reduction of Caspase-3^{+} OPC cell death and increase in MBP^{+} differentiation in the mutant cells (N=3). **D-E**, Quantification of OPC cell death and differentiation in presence of treatment by apo-TF and DFO (N=3-4). **F**, Quantification of ROS assay, in presence of chelation treatment by apo-TF and DFO (N=3-4). **G**, Out of the two lipophilic antioxidants BHT and Trolox that showed efficacy in rescuing mutant OPC differentiation, Trolox also reduced mutant cell death. A lipid oxidizing agent cumene hydroperoxide reversed the beneficial effect by apo-TF (N=3-5).

Supplementary Figure 5. Related to Figure 7. *In vivo* Iron chelation rescues *Jimpy* oligodendrocytes. A-B, Representative images of WT and *Jimpy* primary OPCs treated with vehicle or DFO. **C,** Kaplan-Meyer survival curve of DFP-treated *Jimpy* mice shows a significant increase of lifespan by DFP treatment ($p = 0.047$, N=7 treated group, N=11 untreated group). **D,** Complete blood counts (CBC) for determination of DFP dose. All parameters in CBC showed a dose-dependent anemic effect. A clinically relevant 30mg/kg was chosen with one week break for DFP *in vivo* experiment. **E,** Brains of *Jimpy* mice treated with vehicle or 30mg/kg/day DFP were collected at postnatal day 28 and cerebellar white matter was analyzed for reactive astrocytes (GFAP) and microglia (Iba1) activation. **F,** Quantification showed a significant reduction in inflammatory response in DFP-treated mice (N=3). **G-J,** Fluorescent in situ hybridization (RNA scope) showed a significant reduction in *Atf4* and *Chop* gene expressions in PDGFRα+ OPC after a 7-day *in vivo* DFP treatment from P7 in *Jimpy* mice (N = 3-4).

Supplementary Table 1. Related to STAR Methods. *List of primer sequences for quantitative PCR.*